Int. J. Cancer: **116,** 243–252 (2005)

CD13 (aminopeptidase N) can associate with tumor-associated antigen L6 and enhance the motility of human lung cancer cells

Yu-Wen Chang[1], Shu-Chuan Chen[1], Ee-Chun Cheng[1], Ya-Ping Ko[1], Yi-Chieh Lin[1], Yu-Rong Kao[2], Yeou-Guang Tsay[3], Pan-Chyr Yang[1,4], Cheng-Wen Wu[2] and Steve R. Roffler[1]*

[1]*Institute of Biomedical Sciences, Academia Sinica, Taipei, Taiwan*
[2]*National Health Research Institutes, Taipei, Taiwan*
[3]*Department of Clinical Medicine Research, National Taiwan University Hospital, Taipei, Taiwan*
[4]*Department of Internal Medicine, National Taiwan University Hospital, Taipei, Taiwan*

Cancer metastasis is a multiple-step process that involves the regulated interaction of diverse cellular proteins. We recently reported that the expression of tumor-associated antigen L6 (TAL6) promoted the invasiveness of lung cancer cells and was inversely correlated with disease-free survival of squamous lung carcinoma patients. We now report that CD13 (aminopeptidase N) can associate with TAL6 and can enhance cancer cell migration. CD13 was shown by coimmunoprecipitation to associate *in vitro* with TAL6 on several cancer cell lines and to associate *in vivo* by antibody-mediated copatching immunofluorescence. CD13 was selectively expressed on highly invasive CL1-5 lung cancer cells as compared to poorly invasive CL1-0 lung cancer cells. The role of CD13 aminopeptidase activity in regulating cell motility was investigated with chemical inhibitors, specific antibodies and a catalytically inactive CD13 protein. Inhibition of CD13 aminopeptidase activity by nontoxic concentrations of leuhistin modestly decreased the migration of CL1-5 cells. In contrast, binding of CD13 by specific antibodies significantly reduced both the migration and the invasion of CL1-5 cells. Poorly invasive CL1-0 cells that stably expressed CD13 displayed significantly ($p \leq 0.0005$) enhanced cell migration (300% of control). Expression of an enzymatically inactive CD13 mutant on CL1-0 cells also significantly ($p \leq 0.0005$) enhanced cell migration (200% of control). Our results show that TAL6 and CD13 can form a complex on lung cancer cells, that these molecules can modulate cell migration and invasion and that the influence of CD13 on cell motility did not strictly depend on its aminopeptidase activity.

Key words: tumor-associated antigen L6; CD13; aminopeptidase N; tetraspanin; metastasis; invasion; motility; migration; TAL6

Although tumor cell metastasis is responsible for the majority of cancer deaths, the metastatic process is still poorly understood. Metastasis consists of multiple steps, including altered intra- and intercell adhesion, directed proteolysis and migration, intravasation into the blood circulation or lymph nodes, subsequent attachment to endothelial cells followed by extravasation, invasion and induction of angiogenesis.[1] Tumor-associated antigen L6 (TAL6),[2] originally identified by an antibody that selectively bound to human lung adenocarcinoma,[3] is widely distributed on the majority of human lung, colon, breast and ovarian tumors[3] as well as on renal cell carcinomas[4] and prostate carcinoma cells.[5] Due to its selective tumor expression pattern, TAL6 is a target for cancer immunotherapy,[6] radioimmunotherapy[7] and antibody-directed enzyme prodrug activation.[8] mAb L6 can modulate the motility of human keratinocytes.[9] We recently showed that TAL6 was involved in lung cancer invasion and that TAL6 expression was inversely correlated with the prognosis of lung cancer patients.[10]

Although TAL6 shares topologic features with members of the tetraspanin superfamily, recent analysis suggests that TAL6 belongs to a new transmembrane-4 superfamily comprising TAL6, IL-TMP, TM4SF5 and L6D.[11] The biologic properties of this superfamily remain largely unknown. In the present study, we examined possible interactions between TAL6 and other cell surface molecules in the CL1 lung cancer model. CL1-5 cells were derived from a poorly differentiated lung adenocarcinoma cell line (CL1-0) by selecting cells that displayed enhanced invasiveness in a transwell invasion chamber.[12] CL1-5 cells display increased invasiveness *in vitro*, greater metastatic potential in SCID mice[12] and enhanced invasiveness in a tracheal graft assay.[13] CL1-5 cells were also more malignant than CL1-0 cells in a SCID mouse experimental metastasis model.[10] Here we report that TAL6 can associate with aminopeptidase N (CD13). Functional characterization of CD13 on CL1-5 human lung carcinoma cells indicates that CD13 can enhance cell migration.

Material and methods

Cell lines

Human lung adenocarcinoma cell lines with different invasive and metastatic capabilities (CL1-0 and its subline CL1-5) have been described.[10,12] HT1080 human fibrosarcoma cells and PC-3 human prostate adenocarcinoma cells were obtained from the American Type Culture Collection (Manassas, VA). Hut125 human lung adenocarcinoma cells were obtained from the Veterans General Hospital Cell Bank (Taipei, Taiwan). The cells were free of mycoplasma as determined by a PCR-based mycoplasma detection kit (American Type Culture Collection). The effect of antibodies (20 μg/ml) on the growth of CL1-5 cells was determined by counting the cells in triplicate wells every 24 hr. Doubling times were calculated by linear regression analysis.

Antibodies and recombinant proteins

Anti-TAL6 (L6-20-4), anti-influenza virus (HB65), antirat CD8 (OX8) and antihuman α-fetoprotein (3.3) were prepared as described.[10,14] Monoclonal antibody (mAb) WM15 (NaN_3-free) was purchased from Biodesign International (Saco, ME). mAbs against human CD13 were produced by immunizing BALB/c mice with CL1-5 cells as previously described.[15] FITC-conjugated goat antimouse and rhodamine-conjugated goat antirabbit antibodies were from Organon Teknika (Durham, NC). FITC-conjugated goat antimouse IgG_{2a}-specific antibody was from Serotec (Oxford, U.K.). Biotin-labeled anti-FLAG M2 antibody and HRP-conjugated extravidin were from Sigma Chemical (St. Louis, MO). The extracellular portion of human CD13 (sCD13) and human β-glucuronidase (hβG) were produced as described.[16]

Abbreviations: ECM, extracellular matrix; GAM, goat antimouse antibody; GAR, goat antirabbit antibody; mAb, monoclonal antibody; sCD13, soluble recombinant CD13; TAL6, tumor-associated antigen L6; TM4SF, transmembrane-4 superfamily.

Grant sponsor: Metastasis Program Project Grant, the National Health Research Institutes, Taipei, Taiwan; Grant number: PA-092-CB-06.

***Correspondence to:** Institute of Biomedical Sciences, Academia Sinica, Yen Geo Yuan Road, Section 2, No. 128, Taipei, Taiwan. Fax: +886-2-2782-9142. E-mail: sroff@ibms.sinica.edu.tw

Received 5 July 2004; Accepted after revision 30 December 2004
DOI 10.1002/ijc.21089
Published online 5 April 2005 in Wiley InterScience (www.interscience.wiley.com).

Plasmid construction

The full-length TAL6 cDNA[12] was inserted into the eukaryotic expression vector pCMV-Tag2B (Stratagene, La Jolla, CA) to create pFlag-TAL6 with an N-terminal FLAG tag. Human syntenin 2 was amplified by PCR using cDNA prepared from CL1-5 cells with primers P1, 5′-TGAGAAGAATTCATGTCATCCCTG-TACCCATCTCTA-3′, and P2, 5′-CCTGTGGGGTAGGGTC-TACGGACTGAGCTCACGTCC-3′. The PCR product was digested with *Eco*RI and *Xho*I and then inserted into pCMV-Tag2B to create pflag-syntenin with an N-terminal FLAG tag. Human CD13 was amplified by PCR using cDNA prepared from CL1-5 cells with primers P3, 5′-GCCGCCTCGAGACCATCAC-CATGGCCAAGGGC-3′, and P4, 5′-TTCAAGTCGACGGGAC-TATTTGCTGTTTTCTG-3′. The PCR product was digested with *Xho*I and *Sal*I and then inserted into retroviral vector pLNXC2 (BD Biosciences, San Diego, CA) to create pLNCX2-CD13. The active site glutamic acid (E388) in CD13 was mutated to alanine with the QuickChange Site-Directed Mutagenesis Kit (Stratagene) to produce pLNCX2-mCD13.

Transfection

BALB/3T3 fibroblasts were transiently transfected using lipofectamine 2000 (Gibco Laboratories, Grand Island, NY). CL1-0 cells that stably expressed CD13 or mCD13 were created by infecting CL1-0 cells with recombinant retroviral particles that were packaged by cotranfection of GP2-293 cells (BD Biosciences) with pVSV-G (BD Biosciences) and pLNCX2-CD13 or pLNCX2-mCD13. Cells were selected in G418 and sorted for expression of CD13 on the cells with an FACSAdvantage SE (Becton-Dickinson, Mountain View, CA).

Immunoprecipitation

CL1-5 cells (1.5×10^6) were labeled with 150 μCi/ml ^{35}S-methionine/cysteine (Amersham Biosciences, Piscataway, NJ) in methionine- and cysteine-free medium for 16 hr. The cells were harvested and membrane proteins were solubilized in 150 μl ice-cold solubilization buffer (20 mM Tris-HCl, pH 7.6, 150 mM NaCl, 1 mM $CaCl_2$, 1 mM $MgCl_2$, 0.02% NaN_3 with protease inhibitors) containing 1% Brij-96 for 1 hr on ice. The cells were centrifuged at 100,000*g* for 45 min and the supernatant was precleared by addition of mAb 3.3 and protein A gel. The supernatant was collected and mixed with specific or control mAb for 60 min followed by addition of protein A gel overnight. The protein A beads were extensively washed with ice-cold solubilization buffer containing 1% Brij-96. The beads were then boiled in 50 μl reducing SDS-PAGE buffer and samples were electrophoresed on a gradient SDS-PAGE. The polyacrylamide gel was soaked in Enhance solution for 60 min, washed in water and dried before performing autoradiography.

Large-scale immunoprecipitation of TAL6-associated proteins was performed by first douncing 10^8 CL1-5 cells in 1.5 ml lysis buffer (10 mM Hepes, pH 7.9, 1.5 mM $MgCl_2$, 10 mM KCl, 0.5 mM DTT with protease inhibitors). Nuclei were pelleted by centrifugation at 1,000*g* for 10 min. An aliquot (165 μl) of cytosol buffer (0.3 mM Hepes, pH 7.9, 1.4 M KCl and 30 mM $MgCl_2$) was added to the supernatant, which was then centrifuged at 100,000*g* for 60 min to pellet cellular membranes. The membranes were solubilized and immunoprecipitated with mAb L6 as described above. Samples were electrophoresed on an SDS-PAGE and specific proteins were identified by mass spectrometric analysis.

Combined immunoprecipitation and immunoblotting was performed by first immunoprecipitating TAL6 from solubilized cell membranes or immunoprecipitating CD13 from 3T3 fibroblasts that had been cotransfected with pLNCX2-CD13 and pflag-TAL6. The immunoprecipitates were resolved by SDS-PAGE, transferred to a PVDF membrane and then immunoblotted with rabbit anti-CD13 serum and horseradish peroxidase-conjugated goat antirabbit antibody for CL1-5 cells or biotin-conjugated anti-FLAG M2 antibody and horseradish peroxidase-conjugated extravidin for 3T3 transfectants. Specific bands were visualized by ECL detection according to the manufacturer's instructions (Pierce, Rockford, IL).

In-gel digestion and mass spectrometric analysis

Excised gel pieces were subjected to reduction, pyridylethylation and tryptic digestion (Promega, Madison, WI) as previously described.[17] Multiple peptide sequences were determined on an ABI 140D (Perkin Elmer, Boston, MA) capillary reversed-phase chromatograph that was directly coupled to an LCQ quadruple ion trap mass spectrometer (Thermo Electron, Mountain View, CA) equipped with a standard electrospray source. Interpretation of the MS/MS spectra was performed by database correlation with the algorithm SEQUEST.[18]

Flow cytometric assay

Immunofluorescence staining of cells was performed as described.[19] Mean fluorescence, measured on an FACSCaliber flow cytometer (Becton-Dickinson), was calculated with FlowJo 3.2 (Tree Star, San Carlos, CA).

PCR detection of L6 and CD13

A 634 bp cDNA product of human TAL6 was amplified with primers P1, 5′-CCT AGGGATCCACCATGTGCTATGGGAA GTGTGCA-3′, and P2, 5′-GGGTTGTCTAGATTAGCAGTCA-TATTGCTGTTGGTG-3′, by PCR from cDNA prepared from CL1-0 and CL1-5 cells as described.[14] A 766 bp cDNA fragment of human CD13 was amplified with the primers P3, 5′-AGAACGCCAACAGCTCCCCCG-3′, and P4, 5′-TGCCTGCTT-CTCCACGTAGTC-3′. Likewise, a 324 bp fragment of human CD13 was amplified with the primers P3 and P5, 5′-GGCTGG-GAGCCTCCCACACCA-3′. A 1 kbp fragment of GAPDH was amplified as described.[20] A negative control reaction was performed with all the primers but without polymerase. Ten cycles of touchdown PCR were performed in 2°C intervals from 65 to 55°C followed by 20 cycles at 55°C.

Antibody-mediated copatching

CL1-5 cells were cultured on glass coverslips overnight before they were sequentially stained with 10 μg/ml mAb L6 or mAb HB65, 20 μg/ml FITC-conjugated goat antimouse IgG_{2a}, 5 μg/ml rabbit anti-CD13 or rabbit anti-AFP followed by 6 μg/ml rhodamine-conjugated goat antirabbit antibody. A control murine antibody (5 μg/ml) was added with the rhodamine conjugate to block possible crossreaction between the rhodamine-conjugated goat antirabbit antibody and mAb L6. In some experiments, a murine IgG_{2a} control antibody (5 μg/ml) was added with rabbit anti-CD13 antibody to block possible crossreaction between the CD13 antibody and FITC-conjugated goat antimouse IgG_{2a}. The cells were then fixed with methanol at −20°C for 5 min, followed by acetone at −20°C for 2 min. The coverslips were mounted on slides with 50% glycerol in PBS. Images were obtained on a Bio-Rad MRC 1000 Laser scanning confocal microscope. Sections of cells were collected at 100× magnification (124 × 82 μm). Images were reassembled and overlaid using the shareware Confocal Assistant 4.02 (ftp://ftp.genetics.bio-rad.com/public/confocal/cas).

CD13 activity

CD13 activity on cells was measured by incubating 3.6×10^4 cells in 180 μl PBS with 20 μl ala-p-nitroanilide (20 mM) for 1 hr at 37°C. The effect of anti-CD13 antibodies on CD13 activity was determined by incubating 10 μg BSA, graded amounts of antibody and 0.06 μg sCD13 in 180 μl PBS for 1 hr at 37°C before addition of 20 μl of 20 mM ala-p-nitroanilide for 1 hr at 37°C. The absorbance of the wells was measured at 405 nm. The inhibition of CD13 activity was calculated as percentage CD13 activity relative to wells that were not treated with antibody. All assays were performed in triplicate.

Chemical inhibition of CD13 activity

Graded concentrations of actinonin, bestatin and leuhistin were prepared in cell culture medium and immediately added to CL1-5 cells or incubated at 37°C for 48 hr before addition to CL1-5 cells to determine the stability of the inhibitors. Then 20 μl ala-p-nitroanilide (20 mM) was added to the cells (180 μl) in 96-well microtiter plates for 1 hr at 37°C before the absorbance at 405 nm was measured. The effect of the inhibitors on cell proliferation was assessed by incubating CL1-5 cells (4×10^4) with graded concentrations of the inhibitors for 48 hr before 1 μCi ^{3}H-thymidine was added to the wells for 16 hr. The cells were then harvested and the radioactivity was measured on a TopCount Microplate Scintillation Counter (Packard, Meriden, CT).

CD13 ELISA

The wells of high-protein binding microtiter plates were coated with 0.5 μg sCD13 in PBS overnight at 4°C. The plates were blocked with 2% skim milk before graded amounts of antibody in 50 μl PBS containing 0.1% BSA were added for 1 hr at 37°C. Antibody binding was detected by measuring absorbance at 405 nm after sequential addition of horseradish peroxidase-conjugated goat antimouse antibody and substrate as described.[21]

Matrigel digestion

A 50 μg sample of matrigel was mixed with or without 2 μg sCD13 in a total volume of 30 μl buffer (50 mM Tris-HCl, pH 8.0) for 24 hr at 37°C. Samples were resolved in a 3–8% gradient SDS-PAGE and stained with Coomassie Blue G-250.

Adhesion assay

Adhesion of CL1-5 cells to fibronectin, laminin, vitronectin, collagen type I, or collagen type IV was measured in 3–7 independent assays, each containing 8 replicates as described.[10] Blocking experiments employed 10 μg/ml L6, 4B8, 9A1, 1F4, or control OX8 antibodies.

In vitro *migration and invasion assays*

Tumor cell migration and invasion were examined in a membrane invasion culture system as described with some modifications.[10] Briefly, BD Falcon HTS FluoroBlok 24-Multiwell Insert Systems with 8 μm pores (BD Biosciences) were coated with 5 mg/ml BD Matrigel Basement Membrane Matrix (BD Biosciences) for invasion assays or 100 μg/ml gelatin (Sigma Chemical) for migration assays. Cells (2.5×10^4 for invasion and 5×10^4 for migration) were seeded into the upper wells in RPMI medium containing 10% NuSerum (BD Biosciences). Antibodies were then added at 20 μg/ml to the upper well of the culture system. sCD13 or hβG was added in some experiments to a final concentration of 1 or 10 μg/ml. To cluster 4B8, 1 μg/ml mAb 4B8 was added to CL1-5 cells for 15 min, followed by addition of 10 μg/ml antimouse or antirabbit antibodies. The number of cells passing through the membrane in 6 hr (migration) or 24 hr (invasion) was determined by fixing the membranes with methanol, staining the cells with propidium iodide and counting the cells under a fluorescence microscope. Each experiment contained triplicate wells and was performed 3–7 times.

Statistical analysis

Statistical significance of differences between mean values was estimated by Excel (Microsoft, Redmond, WA) using the independent *t*-test for unequal variances.

Results

CD13 can coimmunoprecipitate with TAL6 in lung cancer cells

To examine whether TAL6 associates with other proteins on the surface of lung cancer cells, CL1-0 and CL1-5 cells were labeled with ^{35}S-methionine/^{35}S-cysteine before the cells were solubilized with Brij 96 and immunoprecipitated with mAb L6 or control antibody. Figure 1(*a*) shows that more TAL6 was immunoprecipitated from highly invasive CL1-5 cells as compared with low invasive CL1-0 cells as expected from the relative expression of TAL6 on these cells.[10] Two additional specific bands were coimmunoprecipitated from CL1-5 cells but not from CL1-0 cells (Fig. 1*a*, upper arrow). We performed large-scale immunoprecipitation of CL1-5 cells with mAb L6 and separated the 2 proteins by SDS-PAGE. The proteins were subjected to in-gel digestion and mass spectrometric analysis. We were unable to identify the lower band, but peptides isolated from the upper band corresponded to human CD13/aminopeptidase N (Fig. 1*b*).

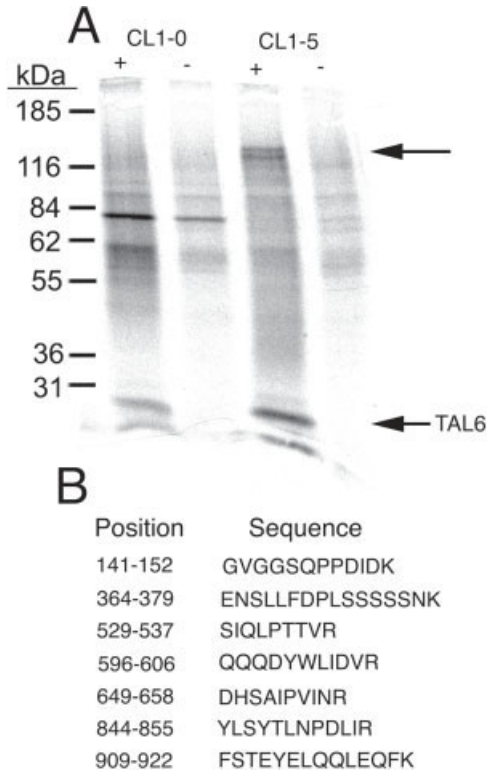

Figure 1 – Immunoprecipitation of CD13 with TAL6. (*a*) Membranes isolated from ^{35}S-methionine/cysteine-labled CL1-0 and CL1-5 cells were solubilized with detergent, immunoprecipitated with mAb L6 (+) or control mAb (−) and separated by SDS-PAGE. The positions of TAL6 and coimmunoprecipitated upper bands on the X-ray film are indicted with arrows. (*b*) The upper band was subjected to in-gel digestion and mass spectrometric analysis. The positions and sequences of the peptides matching the peptide sequence of human CD13 are indicated.

Polyclonal antibodies raised against sCD13 detected recombinant CD13 and wild-type CD13 present in CL1-5 cell lysates (Fig. 2*a*). We further examined the interaction between TAL6 and CD13 by first immunoprecipitating solubilized CL1-5 cells with anti-TAL6 (mAb L6) and then immunoblotting for the presence of CD13. Figure 2(*b*) shows that anti-CD13 mAb 4B8, as a positive control, precipitated a specific band corresponding to endogenous CD13. mAb L6 also coimmunoprecipitated CD13, verifying that TAL6 associates with CD13 on CL1-5 cells. Control antibody OX8 did not precipitate CD13, showing that the L6 antibody immunoprecipitation reaction was specific. We wished to verify the association between TAL6 and CD13 by determining whether TAL6 was present in the immunoprecipitate formed by an anti-CD13 antibody. mAb L6, however, does not bind TAL6 on immunoblots. We therefore introduced a FLAG tag at the N-terminus of TAL6 and then cotransfected murine fibroblasts with pLNCX2-CD13 and pflag-TAL6. As a control, fibroblasts were cotrans-

fected with pLNCX2-CD13 and pflag-syntenin. Immunoblotting of cell lysates with anti-FLAG or anti-CD13 antibodies demonstrated that the transfected cells expressed similar levels of FLAG-TAL6 or FLAG-syntenin and CD13, respectively (Fig. 2*c*). Immunoprecipitation of the solubilized cell membranes with anti-CD13 antibody followed by immunoblotting of the electrophoresed proteins with anti-FLAG antibody demonstrated the presence of FLAG-TAL6 (Fig. 2*d*). Coimmunoprecipitation of FLAG-TAL6 and CD13 was specific because FLAG-syntenin did not coimmunoprecipitate with CD13. Thus, CD13 and TAL6 coimmunoprecipitated with each other in a specific fashion. To examine if CD13 and TAL6 also formed a complex on other cells, we performed coimmunoprecipitation experiments with Hut-125 lung adenocarcinoma cells, HT1080 fibrosarcoma cells and PC-3 prostate adenocarcinoma cells. Figure 2(*e*) shows that CD13 was coimmunoprecipitated by mAb L6 in these cell lines, demonstrating that CD13 association with TAL6 is not limited to a single cell line.

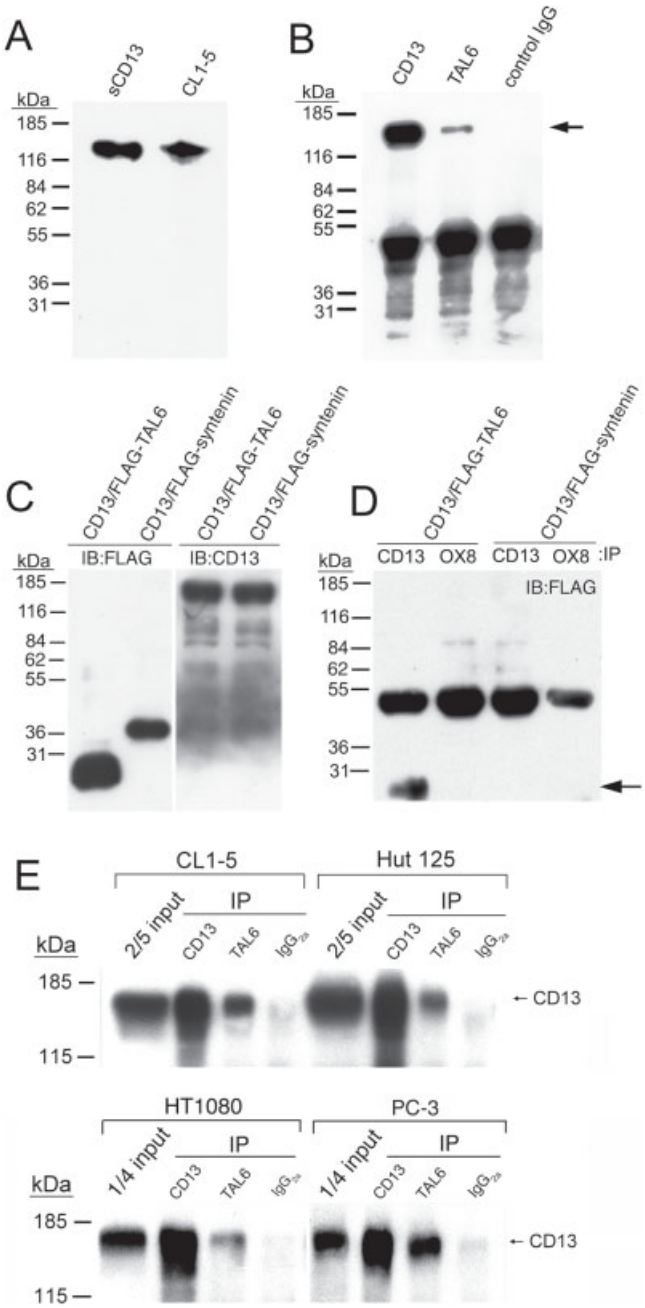

FIGURE 2 – Coimmunoprecipitation of TAL6 and CD13 from lung cancer cells. (*a*) Recombinant sCD13 or CL1-5 cells were separated by SDS-PAGE, transferred to a PVDF membrane and probed with rabbit anti-CD13 immune serum. (*b*) Membranes isolated from CL1-5 cells were solubilized with Brij 96 and then immunoprecipitated with anti-CD13, anti-TAL6, or control antibody. The immunoprecipitates were separated by SDS-PAGE, transferred to a PVDF membrane and probed with rabbit anti-CD13 immune serum. The arrow indicates the position of CD13. (*c*) 3T3 fibroblasts were cotransfected with pLNCX2-CD13 and pflag-TAL6 or PLNCX2-CD13 and pflag-syntenin. Cells were separated by SDS-PAGE, transferred to a PVDF membrane and probed with anti-FLAG antibody (left) or rabbit anti-CD13 immune serum (right). (*d*) Membranes were isolated from the transfected cells in (*c*), solubilized and then immunoprecipitated with anti-CD13 or control OX8 antibody. The immunoprecipitates were separated by SDS-PAGE, transferred to a PVDF membrane and probed with anti-FLAG antibody. The arrow indicates the position of FLAG-TAL6. (*e*) Membranes isolated from CL1-5, Hut-125, HT1080 and PC-3 cancer cells were solubilized and then immunoprecipitated with anti-CD13, anti-TAL6, or control IgG_{2a} antibody. The immunoprecipitates were separated by SDS-PAGE, transferred to a PVDF membrane and probed with rabbit anti-CD13 immune serum. Cell lysate samples corresponding to 2/5 or 1/4 of the total cell lysate input used for immunoprecipitation were also immunoblotted for CD13. The arrow indicates the position of CD13.

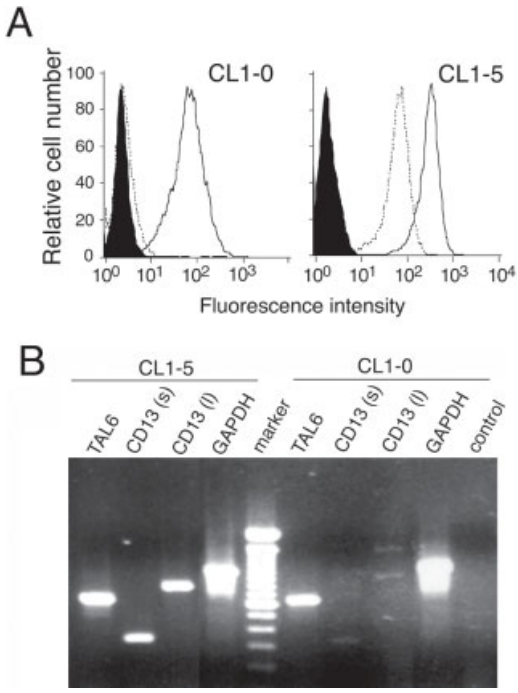

FIGURE 3 – Selective expression of TAL6 and CD13 on CL1-5 cells. (*a*) CL1-0 and CL1-5 cells were stained with anti-TAL6 (solid line), anti-CD13 (dashed line), or control mAb (filled curve) followed by FITC-conjugated goat antimouse IgG before the immunofluorescence of the cells was measured. (*b*) cDNA prepared from CL1-5 (left) or CL1-0 (right) cells was PCR-amplified with primers specific for TAL6, CD13 [324 bp (s) and 766 bp (l), respectively], or GAPDH and electrophoresed on an agarose gel.

CD13 is selectively expressed in a highly invasive cancer cell line

We examined the expression of CD13 on highly invasive CL1-5 cells and poorly invasive CL1-0 cells by flow cytometry analysis. CD13 protein was not detected on CL1-0 cells (Fig. 3*a*, left panel), whereas CL1-5 cells expressed large amounts of CD13 on

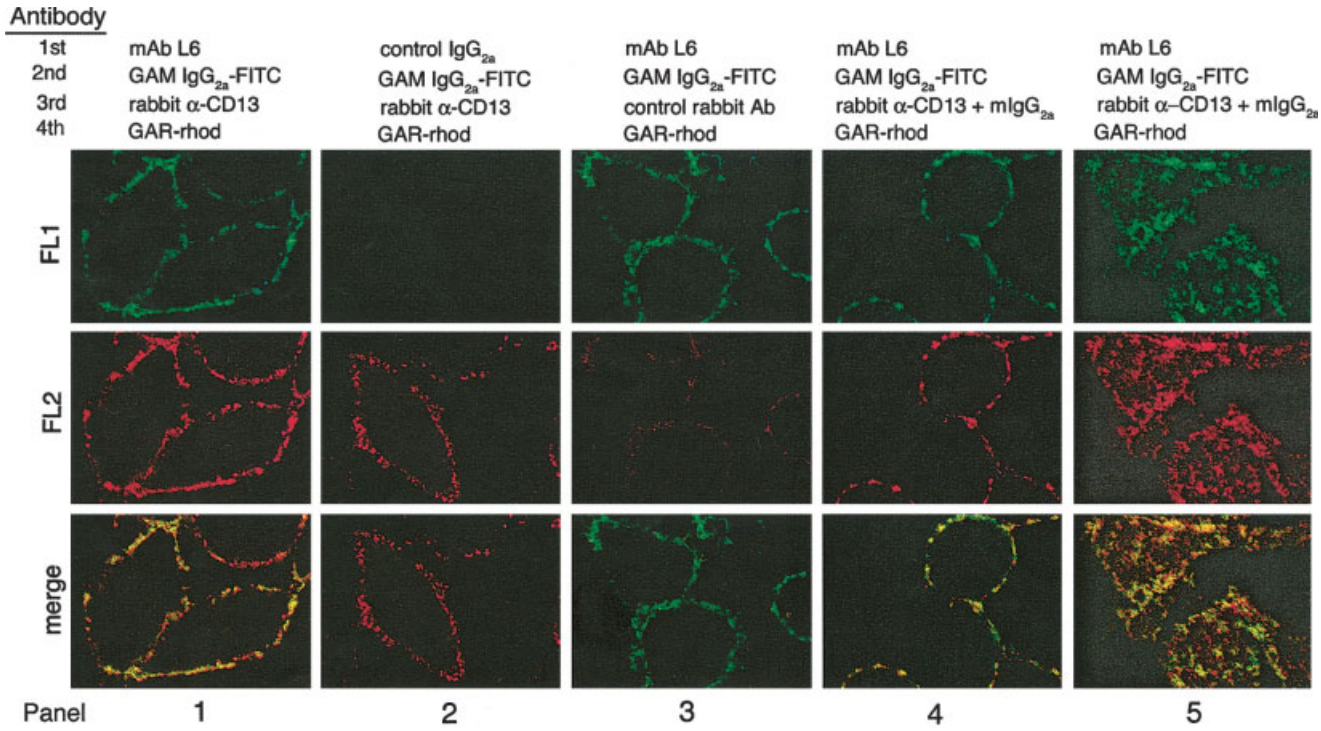

FIGURE 4 – *In vivo* association of TAL6 and CD13 as determined by immunofluorescence copatching. CL1-5 cells were sequentially incubated with mAb L6, FITC-conjugated goat anti-IgG_{2a}, rabbit anti-CD13 and rhodamine-conjugated goat antirabbit antibodies (panel 1). Murine antibody was added during the last staining step to block possible binding of rhodamine-conjugated goat antirabbit antibody to membrane-bound mAb L6. Cells were observed for TAL6 (green), CD13 (red), or merged to visualize colocalization (yellow). Controls were stained and overlaid as in panel 1 except that isotype-matched IgG_{2a} replaced anti-TAL6 (panel 2) or rabbit anti-AFP replaced rabbit anti-CD13 (panel 3). Murine IgG_{2a} was added with rabbit anti-CD13 to block possible binding of anti-CD13 by membrane-bound FITC-conjugated goat anti-IgG_{2a} in panels 4 and 5 (basolateral section).

their surface (Fig. 3*a*, right panel). As previously reported,[10] CL1-5 cells expressed higher levels of TAL6 as compared to CL1-0 cells (Fig. 3*a*). The levels of CD13 mRNA in CL1-0 and CL1-5 cells were also compared by RT-PCR. Figure 3(*b*) shows that CD13 PCR products could be amplified from CL1-5 cells, whereas only trace amounts of CD13 DNA could be amplified from CL1-0 cells, indicating that CD13 mRNA was more highly expressed in the more invasive CL1-5 cells as compared to CL1-0 cells.

In vivo *demonstration of TAL6 and CD13 association by antibody-mediated immunofluorescence copatching*

The association of TAL6 and CD13 on CL1-5 cells *in vivo* was examined by antibody-mediated immunofluorescence copatching.[22] CL1-5 cells were incubated with mAb L6 followed by FITC-labeled polyclonal antibody specific for mouse IgG_{2a} to cluster TAL6 on CL1-5 cells. To determine if CD13 coclustered with TAL6, the cells were incubated with rabbit anti-CD13 serum and rhodamine-labeled antirabbit second antibody. Figure 4 (panel 1) shows green fluorescence representing the staining of TAL6 (top) and red fluorescence indicating the position of CD13 (center). Overlay of the green and red fluorescence revealed considerable colocalization of TAL6 and CD13 as shown by the yellow regions (panel 1, bottom), confirming that CD13 and TAL6 associate *in vivo*. Control overlays demonstrated that staining for CD13 and TAL6 was specific as shown by the lack of yellow fluorescence when mAb L6 was replaced by a control IgG_{2a} mAb (Fig. 4, panel 2) or anti-CD13 antiserum was replaced with control rabbit antibody (Fig. 4, panel 3). The specificity of staining was also demonstrated by the inability of control murine IgG_{2a} to block the binding of anti-CD13 antibody, showing that membrane-bound FITC-conjugated goat antimouse IgG_{2a} did not nonspecifically bind the anti-CD13 antibody (Fig. 4, panels 4 and 5). It should be noted that not all TAL6 and CD13 associated on the cell membrane, as can be appreciated in a basolateral cell section (Fig. 4, panel 5).

CD13-specific monoclonal antibodies can inhibit cancer cell invasion and migration

To investigate a possible role of CD13 in lung cancer invasion, mAbs against CD13 were prepared. The specificity of the antibodies was determined by transfecting murine fibroblasts with pLNCX2-CD13 and staining the cells for specific immunofluorescence. Figure 5(*a*) shows that the commercial anti-CD13 mAb WM15 as well as our anti-CD13 mAbs 9A1, 1F4 and 4B8 bound to fibroblasts that expressed CD13 on their surface, whereas control mAb OX8 did not bind to transfected fibroblasts. The relatively higher fluorescence intensity of cells stained with mAb 1F4 and mAb 4B8 indicates that these antibodies display higher affinities for CD13 as compared to mAb 9A1 and mAb WM15. Figure 5(*b*) compares the binding of the mAbs to recombinant sCD13 as measured by ELISA. All of the new mAbs (9A1, 1F4 and 4B8) bound to recombinant CD13 at least as well as the commercial mAb WM15. Analysis of the influence of the mAbs on the activity of recombinant CD13 showed that WM15 completely inhibited enzymatic activity (Fig. 5*c*). In contrast, both 9A1 and 1F4 maximally inhibited CD13 activity by 50% even at high antibody concentrations, whereas mAb 4B8 did not inhibit CD13 activity.

Figure 6(*a*) shows that inhibition of CD13 catalytic activity with WM15 or 9A1 antibodies did not affect the growth rate of CL1-5 cells as compared to cells treated with control antibody OX8. Likewise, mAb L6 did not inhibit CL1-5 growth. The influence of mAb L6 and anti-CD13 mAbs on the adhesion of CL1-5

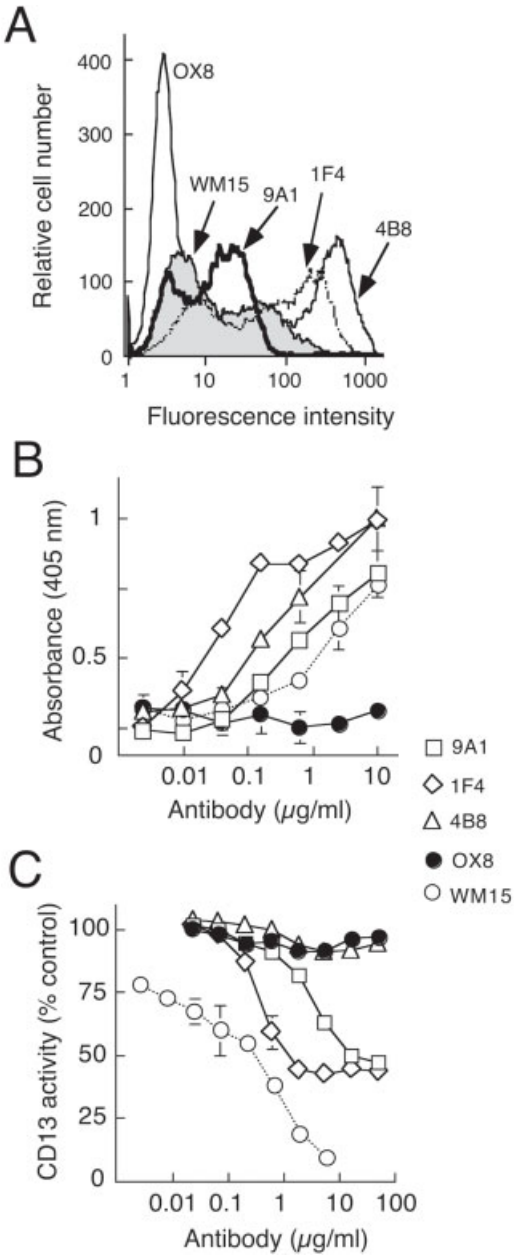

FIGURE 5 – Characterization of anti-CD13 mAbs. (*a*) 3T3 cells were transfected with pLNCX2-CD13 and were then stained with the indicated mAbs and FITC-labeled second antibody before the immunofluorescence intensity of the cells was measured. (*b*) Graded concentrations of the indicated antibodies were incubated in sCD13-coated microtiter plates followed by horseradish peroxidase conjugated second antibody. The mean absorbance of triplicate wells after addition of ABTS substrate is shown. Bars = SE. (*c*) sCD13 (0.3 μg/ml, 0.06 μg) was incubated with graded concentrations of the indicated antibodies for 1 hr before CD13 activity was measured. Results show the mean values of triplicate determinations relative to untreated sCD13. Bars = SE.

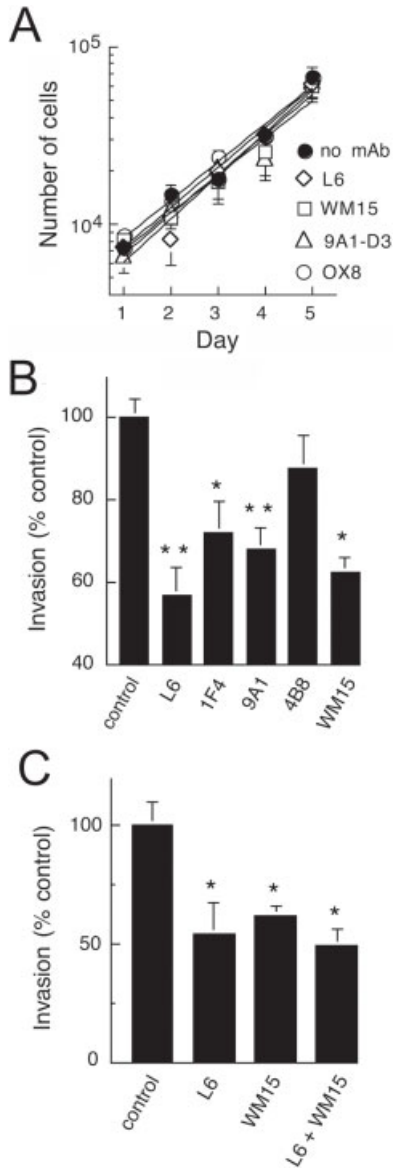

FIGURE 6 – Antibody modulation of CL1-5 cell invasion. (*a*) Triplicate wells of CL1-5 cells incubated without or with 20 μg/ml antibody were counted daily for 5 days. The results show exponential linear regression curves fit to each growth curve. Bars = SE. (*b*) CL1-5 cells were mixed with the indicated mAbs and the number of cells invading through a membrane coated with matrigel was determined. Results show the mean number of invading cells relative to control antibody-treated cells for L6 ($n = 6$), 1F4 ($n = 6$), 9A1 ($n = 3$), 4B8 ($n = 4$) and WM15 ($n = 3$). Bars = SE. (*c*) Invasion of CL1-5 cells treated with L6 and WM15 alone or together is shown relative to control antibody-treated cells ($n = 3$). Bars = SE. Significant differences between control antibody and specific antibody-treated cells are indicated: asterisk, $p \leq 0.05$; double asterisk, $p \leq 0.005$.

cells to purified extracellular matrix proteins was examined. None of the antibodies (L6, 1F4, 4B8 and 9A1) significantly altered the adhesion of CL1-5 cells to fibronectin, laminin, vitronectin, collagen type I, or collagen type IV (results not shown), indicating that TAL6 and CD13 were not involved in the adhesion of CL1-5 cells to the extracellular matrix. To investigate the effect of antibodies on cell invasion, antibodies were added to the upper wells of an invasion chamber containing matrigel-coated membranes. The invasion of CL1-5 cells was determined by counting the number of cells that invaded into the lower chamber. Figure 6(*b*) shows that mAb L6 significantly reduced the invasiveness of CL1-5 cells. All inhibitory anti-CD13 mAbs (1F4, 9A1 and WM15) also significantly inhibited the invasiveness of CL1-5 cells by 30–40%, whereas the noninhibitory mAb 4B8 did not affect CL1-5 invasion as compared to control antibody-treated cells. We also investigated whether addition of antibodies against both TAL6 and CD13 could further reduce CL1-5 invasion. Figure 6(*c*) shows that

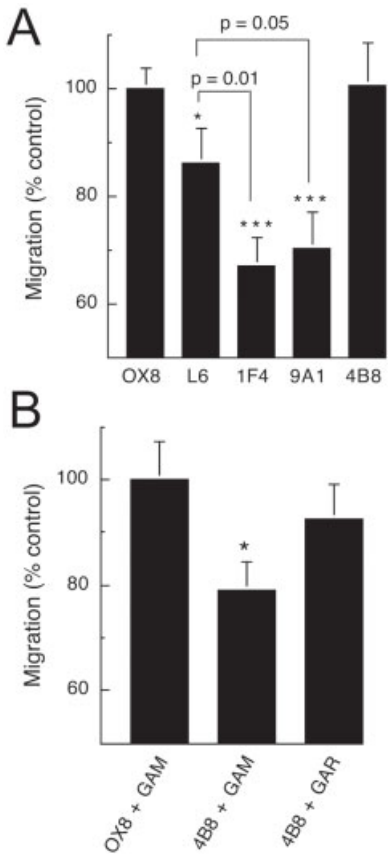

FIGURE 7 – Anti-CD13 antibody modulation of CL1-5 cell migration. (*a*) CL1-5 cells were mixed with 20 μg/ml antibodies and the number of cells migrating through a membrane coated with gelatin was determined. Results show the mean number of migrating cells relative to control antibody-treated cells for L6 ($n = 7$), 1F4 ($n = 5$), 9A1 ($n = 6$) and 4B8 ($n = 5$). Bars = SE. The migration of cells treated with L6, 1F4, or 9A1 was significantly (asterisk, $p \leq 0.05$; triple asterisk, $p \leq 0.0005$) lower than control antibody-treated cells. The migration of cells treated with 1F4 or 9A1 was also significantly lower than cells treated with mAb L6. (*b*) CL1-5 cells were incubated with control antibody (OX8) or anti-CD13 (4B8) followed by crosslinking (GAM) or control (GAR) second antibodies and cell migration was measured. Bars = SE. The migration of cells treated with 4B8 and GAM was significantly (asterisk, $p \leq 0.05$) lower than control antibody (OX8 + GAM)-treated cells.

simultaneous addition of mAb L6 and WM15 did not decrease CL1-5 invasion more than the effect produced by either antibody alone.

The influence of antibodies on cell migration was measured by adding antibodies to CL1-5 cell in the upper wells of a migration chamber and then measuring the number of cells that migrated to the lower chamber within 6 hr. Figure 7(*a*) shows that the addition of mAb L6 to the migration chamber significantly ($p \leq 0.05$) reduced the migration of CL1-5 cells (86% ± 6.4% of control) as compared to CL1-5 cells treated with control mAb OX8 (100% ± 3.8%). Addition of mAb 1F4 or 9A1 to the cells also significantly inhibited CL1-5 migration (67% ± 5.3% and 70% ± 6.7% of control migration, respectively). Although mAb 4B8 did not significantly inhibit the migration of CL1-5 cells, clustering of mAb 4B8 on CL1-5 cells with goat antimouse polyclonal antibody significantly inhibited CL1-5 cell migration (Fig. 7*b*). Crosslinking CD13 with mAb 4B8 and secondary antimouse antibody did not affect the aminopeptidase activity of CD13 (results not shown), suggesting that CD13 aminopeptidase activity may not be absolutely required for modulation of CL1-5 cell motility.

CD13 enzymatic activity was not mandatory for modulation of cancer cell migration

We employed chemical aminopeptidase inhibitors to elucidate the role of CD13 enzymatic activity in the modulation of cell motility and invasion. Because nonspecific suppression of cell growth could artificially reduce cell migration and invasion, the maximum nontoxic doses of 3 aminopeptidase inhibitors were determined. Figure 8(*a*) shows that high concentrations of the inhibitors were toxic to CL1-5 cells as measured by incorporation of radiolabeled thymidine into cellular DNA. The maximum nontoxic concentration of each inhibitor was judged to be 1, 8 and 1 μg/ml for actinonin, bestatin and leuhistin, respectively. CD13 activity on CL1-5 cells, as measured by the cleavage of ala-p-nitroanilide, was inhibited by about 70%, 40% and 70% for actinonin, bestatin and leuhistin at these concentrations, respectively (Fig. 8*a*). These levels of inhibition were comparable to the inhibition of CD13 activity produced by mAb 1F4 and mAb 9A1. The inhibitors were stable for 2 days in culture medium (greater than the length of the invasion assay) because similar inhibition of CD13 activity was measured after the inhibitors were incubated in culture medium for 48 hr (Fig. 8*a*). The effect of the inhibitors on the *in vitro* migration and invasiveness of CL1-5 cells was examined in a transwell system. Actinonin inhibited the migration of CL1-5 cells by 12% ($p = 0.051$) and leuhistin inhibited the migration of CL1-5 cells by 14% ($p \leq 0.05$). Bestatin did not alter cell migration (Fig. 8*b*). None of the inhibitors significantly altered the invasion of CL1-5 cells through matrigel-coated membranes (Fig. 8*c*).

The modest effect of the CD13 inhibitors on CL-5 cell migration and invasion as compared to the effects produced by the anti-CD13 antibodies suggested that some of the biologic effects of CD13 could be independent of CD13 aminopeptidase activity. To elucidate the role of CD13 activity on cell migration and invasion, we generated a mutant form of CD13 in which the active site glutamic acid was changed to alanine. Stable populations of fibroblasts and CL1-0 cells were generated that express wild-type or mutant CD13. Murine fibroblasts were employed because they display low endogenous levels of neutral aminopeptidase activity. The expression of CD13 and mCD13 in the cells was determined by immunoblotting with an anti-CD13 antibody. CL1-0 cells did not express detectable CD13 protein (Fig. 9*a*). Stable CL1-0 transfectants, in contrast, expressed high levels of CD13 and mCD13. 3T3 fibroblasts also expressed similar levels of CD13 and mCD13 proteins. We performed immunofluorescence staining to ensure that CD13 and mCD13 were expressed on the surface of the transfected cells. Figure 9(*b*) demonstrates that both 3T3 and CL1-0 transfectants displayed comparable levels of CD13 and mCD13 on their surface. The aminopeptidase activity of the cells was measured by adding aminopeptidase substrate to live cells and measuring the increase in absorbance after 60 min. Figure 9(*c*) shows that cells expressing mCD13 displayed similar aminopeptidase activity as the parental 3T3 or CL1-0 cells, respectively, demonstrating that mCD13 did not possess aminopeptidase activity. In contrast, cells engineered to express wild-type CD13 displayed enhanced aminopeptidase activity as compared to the parental cells. The invasiveness of CL1-0 cells that expressed CD13 or mCD13 was determined in the matrigel invasion assay. Figure 9(*d*) shows that CD13 did not influence the invasiveness of CL1-0 cells. In contrast, expression of CD13 on CL1-0 cells greatly increased the migration of these cells to about 300% of the levels measured in the parental CL1-0 cells or CL1-0 cells that were stably transfected with empty vector (Fig. 9*e*). CL1-0 cells that expressed mCD13 also displayed enhanced migration as compared to the parental CL1-0 cells, although the migration was significantly less than cells expressing enzymatically active CD13. To examine the influence of CD13 on cell migration, a soluble form of CD13 (sCD13) was added with CL1-0 cells in the upper wells of the migration chamber. Soluble CD13 possesses aminopeptidase activity but should lack activities associated with expression on the plasma membrane. Figure 9(*f*) shows that sCD13 significantly

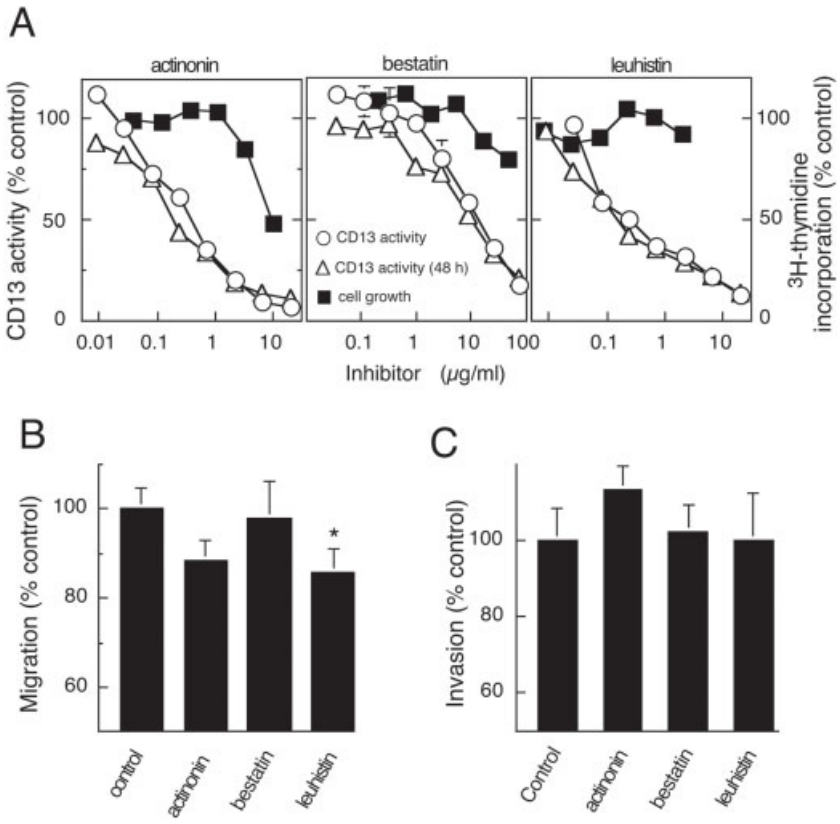

FIGURE 8 – Effect of CD13 inhibitors on CL1-5 cell migration and invasion. (*a*) CL1-5 cells were incubated with the indicated concentrations of actinonin, bestatin, or leuhistin for 48 hr before ^{3}H-thymidine incorporation into cellular DNA was determined (filled square). The CD13 activity of the cells was determined immediately (open circle) or 48 hr (open triangle) after addition of the inhibitors. Results show mean values of triplicate determinations relative to untreated control cells. Bars = SE. (*b*) The migration of CL1-5 cells treated with 1 μg/ml actinonin ($n = 3$), 8 μg/ml bestatin ($n = 3$), or 1 μg/ml leuhistin ($n = 3$) through a polycarbonate membrane relative to the invasion of untreated CL1-5 cells ($n = 3$) is shown. Bars = SE. The migration of cells treated with leuhistin was significantly ($p \leq 0.05$) less than control cells. (*c*) The invasion of CL1-5 cells treated with 1 μg/ml actinonin ($n = 7$), 8 μg/ml bestatin ($n = 7$), or 1 μg/ml leuhistin ($n = 4$) through matrigel relative to the invasion of untreated CL1-5 cells ($n = 7$) is shown. Bars = SE.

increased the migration of CL1-0 cells as compared to a control recombinant protein (hβG) that was produced and purified in an identical manner as sCD13. The degree that sCD13 enhanced CL1-0 cell migration (80%) was similar to the enhancement attributable to active CD13 expressed on CL1-0 cells (90% = the difference between CD13 and mCD13 in Fig. 9*e*). These results show that CD13 can enhance the migration of cancer cells in both aminopeptidase-dependent and aminopeptidase-independent fashions.

Discussion

TAL6 is the prototypical member of a new transmembrane-4 superfamily that includes TAL6, IL-TMP, TM4SF5 and L6D.[11] Although little is known about the biologic function of these proteins, we recently reported that TAL6 can promote cancer cell invasion.[10] TAL6 shares similar topologic characteristics as members of the tetraspanin superfamily, including the presence of transmembrane-4 domains, a small and large extracellular loop, and short cytoplasmic N- and C-terminal domains. Many tetraspanins, which includes CD9, CD63/ME491, CD81/TAPA-1, CD82 and CD151/PETA-3,[23] have been implicated in cancer cell migration and metastasis[24–27] and correlate with the prognosis and survival of cancer patients.[28–30] The biologic activities of tetraspanin proteins are often attributed to their association with integrins and specific surface proteins.[31–33] We therefore tested the hypothesis that TAL6 may also associate with specific integrins or surface receptors. Although we did not find any association between TAL6 and integrins, we did find that TAL6 can associate with CD13/aminopeptidase N on lung cancer cells as well as on prostate adenocarcinoma and fibrosarcoma cells. The association between CD13 and TAL6 was also verified to occur on CL1-5 cells by antibody-mediated immunofluorescence copatching.[22]

CD13 is a zinc-dependent metalloproteinase that is anchored on cells as a type II transmembrane protein.[34] CD13 cleaves neutral amino acids from the N-terminal of hormone peptides such as enkephalin, tuftsin and angiotensin III.[34] CD13 is widely expressed throughout the body but is especially prevalent in the brush border of the intestine and kidney. The expression of CD13 has been correlated with medium survival times of patients with pancreatic cancer[35] and CD13 has also recently been associated with cell motility in thyroid cancers.[36] Epithelial cells in tumors undergoing angiogenesis preferentially express CD13.[37,38] CD13 levels can also be upregulated in response to hypoxia, basic fibroblast growth factor and vascular endothelial growth factor.[39]

CD13 was expressed at high levels on more invasive CL1-5 cells but was not detected on poorly invasive CL1-0 cells, suggesting a casual link with lung cancer cell malignancy. Several studies have reported that CD13 plays a role in the invasion of carcinoma cells.[40–44] Our results, however, support a major role for CD13 in modulating lung cancer cell motility. First, aminopeptidase inhibitors had no effect on the invasion of CL1-5 cells (Fig. 8*c*), whereas actinonin and leuhistin reduced the migration of CL1-5 cells (Fig. 8*b*). Second, expression of CD13 on CL1-0 cells greatly enhanced cell migration (Fig. 9*e*) but had no effect on cell invasion (Fig. 9*d*). Finally, soluble recombinant CD13 significantly promoted the motility of CL1-0 cells (Fig. 9*f*) but had minimal effects on CL1-0 cell invasiveness (results not shown). Although anti-CD13 antibodies modulated both cell migration and cell invasion, the latter effects may have been mediated by TAL6 that was complexed with CD13. Taken together, these results strongly argue that CD13 modulates CL1-0 cell motility rather than cell invasiveness. Our results are in agreement with recent reports demonstrating a role for CD13 in cell motility in endothelial cells and several human carcinoma cell lines.[36,45]

We unexpectedly found that CD13 can promote cell migration independently of its aminopeptidase activity. The strongest evidence that CD13 aminopeptidase activity was not absolutely required for enhanced migration was the finding that expression of a catalytically inactive form of CD13 significantly ($p \leq 0.0005$) enhanced the migration of CL1-0 cells. Expression of catalytically active CD13 further enhanced CL1-0 cell migration, suggesting

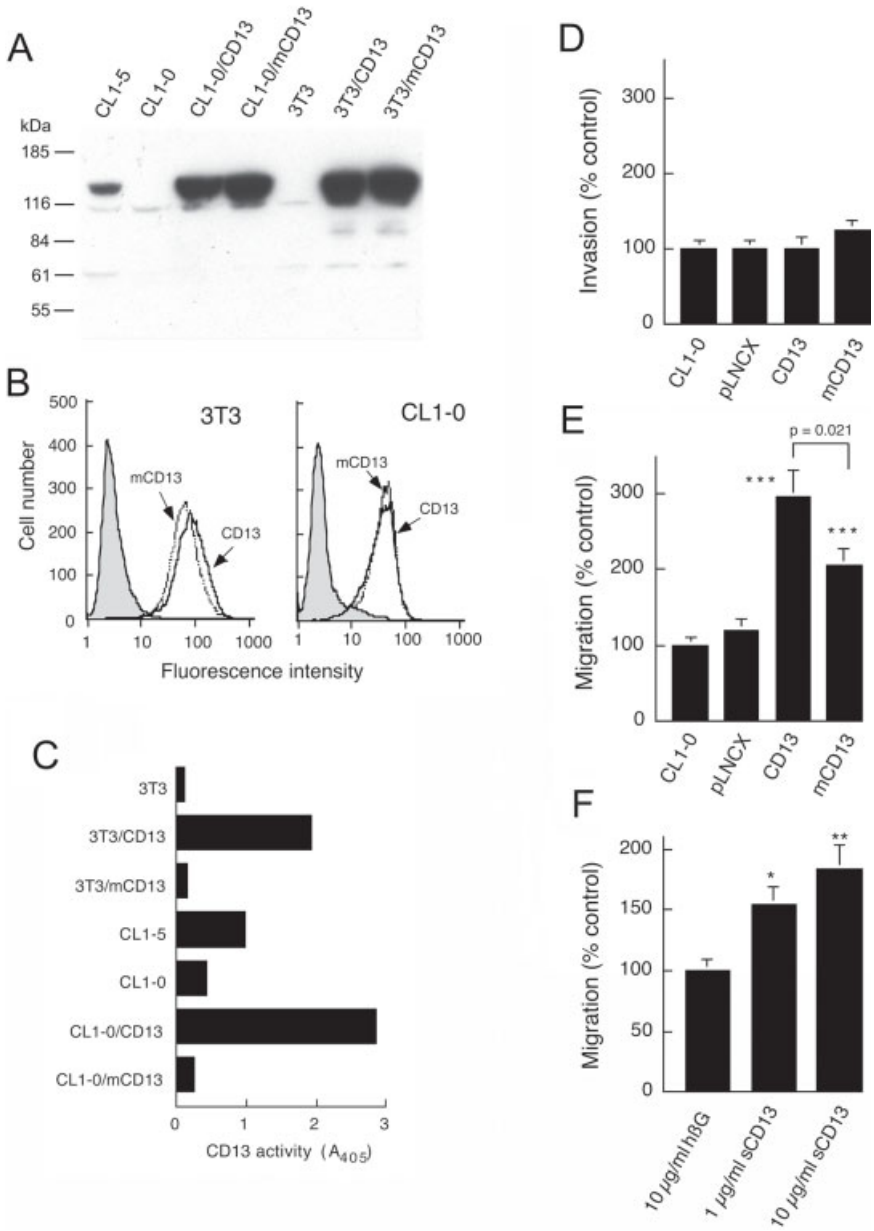

FIGURE 9 – Mutant CD13 can enhance the migration of lung cancer cells. (*a*) CL1-5, CL1-0 and 3T3 cells as well as CL1-0 and 3T3 cells that were stably transfected with pLNCX2-CD13 or pLNCX2-mCD13 were separated by SDS-PAGE, transferred to a PDVF membrane and probed with rabbit anti-CD13 immune serum. (*b*) 3T3 (left) and CL1-0 (right) cells that were stably transfected with pLNCX2-CD13 or pLNCX2-mCD13 were stained with anti-CD13 followed by FITC-conjugated second antibody before the immunofluorescence of the cells was measured. (*c*) The indicated parental and stably transfected cells were incubated with ala-p-nitroanilide for 60 min before the absorbance was measured at 405 nM. Results show mean values of triplicate determinations. Bars = SD. (*d*) The invasion of parental CL1-0 cells and CL1-0 cells that were stably transfected with vector (pLNCX), pLNCX2-CD13, or pLNCX2-mCD13 was determined. Results show the mean number of invading cells (n = 3) relative to control (CL1-0) cells. Bars = SE. (*e*) The migration of parental CL1-0 cells and CL1-0 cells that were stably transfected with vector (pLNCX), pLNCX2-CD13, or pLNCX2-mCD13 was determined. Results show the mean number of migrating cells (n = 3) relative to control (CL1-0) cells. Bars = SE. The migration of CL1-0 cells that expressed CD13 or mCD13 was significantly (triple asterisk, $p \leq 0.0005$) greater than the migration of CL1-0 cells. The migration of CL1-0 cells that expressed CD13 was also significantly ($p = 0.021$) greater than cells that expressed mutant CD13. (*f*) The migration of CL1-0 cells treated with 1 μg/ml sCD13 or 10 μg/ml sCD13 through a polycarbonate membrane relative to the invasion of CL1-0 cells treated with 10 μg/ml hβG (control) is shown. Bars = SE. The migration of CL1-0 cells treated with sCD13 was significantly greater than cells treated with hβG: asterisk, $p \leq 0.01$; double asterisk, $p \leq 0.005$.

that the aminopeptidase-dependent and aminopeptidase-independent functions of CD13 are additive. Some antibodies appeared to be able to induce both aminopeptidase-dependent and -independent inhibition of CL1-5 cell migration. Thus, antibodies that both clustered CD13 on the cell membrane and inhibited CD13 aminopeptidase activity (9A1 and 1F4) produced greater inhibition of cell migration as compared to either inhibition of aminopeptidase activity alone (*i.e.*, chemical aminopeptidase inhibitors) or clustering of CD13 alone (*i.e.*, noninhibitory antibody 4B8). Interestingly, anti-CD13 antibodies have recently been shown to increase intracellular calcium levels and induce the activation of mitogen-activated protein kinases in monocytes.[46] The greater effect on cell migration of CD13 overexpression as compared to antibody or chemical inhibitors likely reflects the relative ineffectiveness of blocking a single molecular pathway in a background of multiple and possibly redundant pathways. Taken together, our results support the notion that CD13 may promote cancer cell migration by both aminopeptidase-dependent and aminopeptidase-independent mechanisms.

In summary, we have shown for the first time that CD13 can associate with TAL6 on cancer cells. CD13 is involved in the motility of lung cancer cells, whereas TAL6 appears to be primarily involved in cell invasion.[10] Thus, CD13 and TAL6 may play nonredundant specialized roles in the TAL6/CD13 molecular complex. The molecular mechanisms responsible for the regulation of cancer cell invasion and migration by the TAL6/CD13 complex as well as possible coregulation of their function by each other are currently under investigation. We also demonstrated that CD13 can enhance cancer cell motility by both aminopeptidase-dependent and aminopeptidase-independent mechanisms. Therefore, our results suggest that therapies based on inhibition of CD13 aminopeptidase activity[47,48] may be less effective than originally anticipated.

Acknowledgements

The authors thank Ms. Ya-Chen Tsai, Ms. Shao-Yu Chen and Mr. Chien-Che Hung for technical assistance.

References

1. Woodhouse EC, Chuaqui RF, Liotta LA. General mechanisms of metastasis. Cancer 80:1529–37.
2. Marken JS, Schieven GL, Hellstrom I, Hellstrom KE, Aruffo A. Cloning and expression of the tumor-associated antigen L6. Proc Natl Acad Sci USA 89:3503–7.
3. Hellstrom I, Horn D, Linsley P, Brown JP, Brankovan V, Hellstrom KE. Monoclonal mouse antibodies raised against human lung carcinoma. Cancer Res 46:3917–23.
4. Svensson HP, Frank IS, Berry KK, Senter PD. Therapeutic effects of monoclonal antibody-beta-lactamase conjugates in combination with a nitrogen mustard anticancer prodrug in models of human renal cell carcinoma. J Med Chem 1998;41:1507–12.
5. O'Donnell RT, DeNardo SJ, Shi XB, Mirick GR, DeNardo GL, Kroger LA, Meyers FJ. L6 monoclonal antibody binds prostate cancer. Prostate 1998;37:91–7.
6. Goodman GE, Hellstrom I, Brodzinsky L, Nicaise C, Kulander B, Hummel D, Hellstrom KE. Phase I trial of murine monoclonal antibody L6 in breast, colon, ovarian, and lung cancer. J Clin Oncol 1990;8:1083–92.
7. Denardo SJ, Richman CM, Goldstein DS, Shen S, Salako Q, Kukis DL, Meares CF, Yuan A, Welborn JL, Denardo GL. Yttrium-90/indium-111-DOTA-peptide-chimeric L6: pharmacokinetics, dosimetry and initial results in patients with incurable breast cancer. Anticancer Res 1997;17:1735–44.
8. Svensson HP, Vrudhula VM, Emswiler JE, MacMaster JF, Cosand WL, Senter PD, Wallace PM. *In vitro* and *in vivo* activities of a doxorubicin prodrug in combination with monoclonal antibody beta-lactamase conjugates. Cancer Res 1995;55:2357–65.
9. Storim J, Friedl P, Schaefer BM, Bechtel M, Wallich R, Kramer MD, Reinartz J. Molecular and functional characterization of the four-transmembrane molecule l6 in epidermal keratinocytes. Exp Cell Res 2001;267:233–42.
10. Kao YR, Shih JY, Wen WC, Ko YP, Chen BM, Chan YL, Chu YC, Yang PC, Wu CW, Roffler SR. Tumor-associated antigen L6and the invasion of human lung cancer cells. Clin Cancer Res 2003;9:2807–16.
11. Wright MD, Ni J, Rudy GB. The L6 membrane proteins: a new four-transmembrane superfamily. Protein Sci 2000;9:1594–600.
12. Chu YW, Yang PC, Yang SC, Shyu YC, Hendrix MJ, Wu R, Wu CW. Selection of invasive and metastatic subpopulations from a human lung adenocarcinoma cell line. Am J Respir Cell Mol Biol 1997;17:353–60.
13. Chen JJ, Peck K, Hong TM, Yang SC, Sher YP, Shih JY, Wu R, Cheng JL, Roffler SR, Wu CW, Yang PC. Global analysis of gene expression in invasion by a lung cancer model. Cancer Res 2001;61:5223–30.
14. Chou WC, Liao KW, Lo YC, Jiang SY, Yeh MY, Roffler SR. Expression of chimeric monomer and dimer proteins on the plasma membrane of mammalian cells. Biotechnol Bioeng 1999;65:160–9.
15. Roffler SR, Chan J, Yeh MY. Potentiation of radioimmunotherapy by inhibition of topoisomerase I. Cancer Res 1994;54:1276–85.
16. Wu CH, Balasubramanian WR, Ko YP, Hsu G, Chang SE, Prijovich ZM, Chen KC, Roffler SR. Simple mammalian cell production of recombinant proteins. Biotechnol Appl Biochem 2004;15:15.
17. Tsay YG, Wang YH, Chiu CM, Shen BJ, Lee SC. A strategy for identification and quantitation of phosphopeptides by liquid chromatography/tandem mass spectrometry. Anal Biochem 2000;287:55–64.
18. Eng JK, McCormick AL, Yates JR. An approach to correlate tandem mass spectral data of peptides with amino acid sequences in a protein database. J Am Soc Mass Spectrom 1994;5:976–89.
19. Liao KW, Chou WC, Lo YC, Roffler SR. Design of transgenes for efficient expression of active chimeric proteins on mammalian cells. Biotechnol Bioeng 2001;73:313–23.
20. Peck K, Sher YP, Shih JY, Roffler SR, Wu CW, Yang PC. Detection and quantitation of circulating cancer cells in the peripheral blood of lung cancer patients. Cancer Res 1998;58:2761–5.
21. Cheng TL, Wu PY, Wu MF, Chern JW, Roffler SR. Accelerated clearance of polyethylene glycol-modified proteins by anti-polyethylene glycol IgM. Bioconjug Chem 1999;10:520–8.
22. Constantinescu SN, Keren T, Socolovsky M, Nam H, Henis YI, Lodish HF. Ligand-independent oligomerization of cell-surface erythropoietin receptor is mediated by the transmembrane domain. Proc Natl Acad Sci USA 2001;98:4379–84.
23. Boucheix C, Rubinstein E. Tetraspanins. Cell Mol Life Sci 2001;58:1189–205.
24. Ikeyama S, Koyama M, Yamaoko M, Sasada R, Miyake M. Suppression of cell motility and metastasis by transfection with human motility-related protein (MRP-1/CD9) DNA. J Exp Med 1993;177:1231–7.
25. Radford KJ, Thorne RF, Hersey P. Regulation of tumor cell motility and migration by CD63 in a human melanoma cell line. J Immunol 1997;158:3353–8.
26. Dong JT, Lamb PW, Rinker-Schaeffer CW, Vukanovic J, Ichikawa T, Isaacs JT, Barrett JC. KAI1, a metastasis suppressor gene for prostate cancer on human chromosome 11p11.2. Science 1995;268:884–6.
27. Testa JE, Brooks PC, Lin JM, Quigley JP. Eukaryotic expression cloning with an antimetastatic monoclonal antibody identifies a tetraspanin (PETA-3/CD151) as an effector of human tumor cell migration and metastasis. Cancer Res 1999;59:3812–20.
28. Miyake M, Nakano K, Itoi SI, Koh T, Taki T. Motility-related protein-1 (MRP-1/CD9) reduction as a factor of poor prognosis in breast cancer. Cancer Res 1996;56:1244–9.
29. Higashiyama M, Taki T, Ieki Y, Adachi M, Huang CL, Koh T, Kodama K, Doi O, Miyake M. Reduced motility related protein-1 (MRP-1/CD9) gene expression as a factor of poor prognosis in non-small cell lung cancer. Cancer Res 1995;55:6040–4.
30. Adachi M, Taki T, Ieki Y, Huang CL, Higashiyama M, Miyake M. Correlation of KAI1/CD82 gene expression with good prognosis in patients with non-small cell lung cancer. Cancer Res 1996;561751–5.
31. Maecker HT, Todd SC, Levy S. The tetraspanin superfamily: molecular facilitators. FASEB J 1997;11:428–42.
32. Indig FE, Diaz-Gonzalez F, Ginsberg MH. Analysis of the tetraspanin CD9-integrin alphaIIbbeta3 (GPIIb-IIIa) complex in platelet membranes and transfected cells. Biochem J 1997;327:291–8.
33. Serru V, Le Naour F, Billard M, Azorsa DO, Lanza F, Boucheix C, Rubinstein E. Selective tetraspan-integrin complexes (CD81/alpha4beta1, CD151/alpha3beta1, CD151/alpha6beta1) under conditions disrupting tetraspan interactions. Biochem J 1999;340:103–11.
34. Riemann D, Kehlen A, Langner J. CD13: not just a marker in leukemia typing. Immunol Today 1999;20:83–8.
35. Ikeda N, Nakajima Y, Tokuhara T, Hattori N, Sho M, Kanehiro H, Miyake M. Clinical significance of aminopeptidase N/CD13 expression in human pancreatic carcinoma. Clin Cancer Res 2003;9:1503–8.
36. Kehlen A, Lendeckel U, Dralle H, Langner J, Hoang-Vu C. Biological significance of aminopeptidase N/CD13 in thyroid carcinomas. Cancer Res 2003;63:8500–6.
37. Pasqualini R, Koivunen E, Kain R, Lahdenranta J, Sakamoto M, Stryhn A, Ashmun RA, Shapiro LH, Arap W, Ruoslahti E. Aminopeptidase N is a receptor for tumor-homing peptides and a target for inhibiting angiogenesis. Cancer Res 2000;60:722–7.
38. Arap W, Pasqualini R, Ruoslahti E. Cancer treatment by targeted drug delivery to tumor vasculature in a mouse model. Science 1998;279:377–80.
39. Bhagwat SV, Lahdenranta J, Giordano R, Arap W, Pasqualini R, Shapiro LH. CD13/APN is activated by angiogenic signals and is essential for capillary tube formation. Blood 2001;97:652–9.
40. Menrad A, Speicher D, Wacker J, Herlyn M. Biochemical and functional characterization of aminopeptidase N expressed by human melanoma cells. Cancer Res 1993;53:1450–5.
41. Fujii H, Nakajima M, Saiki I, Yoneda J, Azuma I, Tsuruo T. Human melanoma invasion and metastasis enhancement by high expression of aminopeptidase N/CD13. Clin Exp Metastasis 1995;13:337–44.
42. Saiki I, Fujii H, Yoneda J, Abe F, Nakajima M, Tsuruo T, Azuma I. Role of aminopeptidase N (CD13) in tumor-cell invasion and extracellular matrix degradation. Int J Cancer 1993;54:137–43.
43. Ishii K, Usui S, Sugimura Y, Yoshida S, Hioki T, Tatematsu M, Yamamoto H, Hirano K. Aminopeptidase N regulated by zinc in human prostate participates in tumor cell invasion. Int J Cancer 2001;92:49–54.
44. Fujii H, Nakajima M, Aoyagi T, Tsuruo T. Inhibition of tumor cell invasion and matrix degradation by aminopeptidase inhibitors. Biol Pharm Bull 1996;19:6–10.
45. Hashida H, Takabayashi A, Kanai M, Adachi M, Kondo K, Kohno N, Yamaoka Y, Miyake M. Aminopeptidase N is involved in cell motility and angiogenesis: its clinical significance in human colon cancer. Gastroenterology 2002;122:376–86.
46. Santos AN, Langner J, Herrmann M, Riemann D. Aminopeptidase N/CD13 is directly linked to signal transduction pathways in monocytes. Cell Immunol 2000;201:22–32.
47. Ichinose Y, Genka K, Koike T, Kato H, Watanabe Y, Mori T, Iioka S, Sakuma A, Ohta M. Randomized double-blind placebo-controlled trial of bestatin in patients with resected stage I squamous-cell lung carcinoma. J Natl Cancer Inst 2003;95:605–10.
48. Shim JS, Lee HS, Shin J, Kwon HJ. Psammaplin A, a marine natural product, inhibits aminopeptidase N and suppresses angiogenesis *in vitro*. Cancer Lett 2004;203:163–9.